Journal of Alloys and Compounds 509 (2011) 2697–2702

Contents lists available at ScienceDirect

Journal of Alloys and Compounds

journal homepage: www.elsevier.com/locate/jallcom

Phase transformations in the B2 phase of Co-rich Co–Al binary alloys

K. Niitsu, T. Omori, M. Nagasako, K. Oikawa, R. Kainuma*, K. Ishida

Department of Materials Science, Graduate School of Engineering, Tohoku University, 6-6-02 Aoba-yama, Sendai 980-8579, Japan

ARTICLE INFO

Article history:
Received 17 May 2010
Received in revised form
17 November 2010
Accepted 22 November 2010
Available online 30 November 2010

Keywords:
Metals
Scanning and transmission electron microscopy
Magnetic measurements

ABSTRACT

Phase transformations in the β (B2) phase of Co–21 and –23 at.% Al alloys were examined using transmission electron microscopy, energy dispersive X-ray spectroscopy and differential scanning calorimetry. The microstructures obtained from as-quenched specimens were found to be strongly affected by the quenching condition. While relatively thick sheet-specimens with a lower quenching rate showed bainitic plate precipitates with a fcc structure, a martensite-like structure was observed by optical microscopy in relatively thin specimens with a higher quenching rate. Regardless of the quenching condition, a spinodal-like microstructure composed of A2 and B2 phases was also detected and the A2 phase changed to a metastable hcp phase during further aging.

1. Introduction

Co–Al is one of the most important binary systems for many Co-based functional alloys, such as hard magnets [1], shape memory material [2,3] and heat-resistant materials [4]. There are three solid phases, namely α-Co (A1: fcc solid solution), ε-Co (A3: hcp solid solution) and β-CoAl (B2: ordered bcc) phases, in the Co-rich portion of the Co–Al binary system, as shown in Fig. 1 [5]. In both the α and β, phases the high solubility at high temperatures remarkably decreases with decreasing temperature at around 800 °C and 1100 °C, respectively. To date, some metastable phases precipitating in these solid-solution phases have been reported. In the α solid-solution aged at 600 °C, a Co_3Al ($L1_2$: ordered fcc) metastable phase appears with a cuboidal microstructure similar to that in the Ni_3Al phase observed in the Ni-based superalloys [6]. On the other hand, very fine ε plates have been confirmed to precipitate into the supercooled β phase at elevated temperatures even in the α + β two-phase region of the phase diagram and to cause a high coercivity [7,8]. This ε + β alloy with high coercivity is known as Malcolloy [1,7,8]. Furthermore, thermodynamic analysis has suggested that metastable phase separation of A2 and B2 phases occurs in the same α + β two-phase region of the phase diagram [9], and actually the metastable A2 phase in β phase alloys has experimentally been confirmed by Kozakai et al. [10] as plotted with open circles in Fig. 1. Recently, the present author's group has experimentally determined the Co–Fe–Al ternary phase diagrams at some elevated temperatures [11] and estimated metastable equilibrium compositions in the A2 + B2 two-phase region of Co–Al binary system by extrapolation from the ternary equilibrium data, as shown by the closed circles in Fig. 1. This suggests that the large α + β two-phase concentration region not including a stable $L1_2$ phase in the Co–Al phase diagram, which is different from the Ni–Al phase diagram, is due to the existence of the A2 + B2 metastable phase equilibrium. In the Co–Al system, there is another important point different from that in the Ni–Al system, which is martensitic transformation induced by quenching from the β phase region [12,13]. Although the Ni-rich β-NiAl alloys are known to show a martensitic transformation from B2 to $L1_0$ (ordered fct) phase [14], no martensitic transformation from the B2 phase has been reported in binary β-CoAl alloys. In the present work, the phase transformations in Co-rich β alloys induced by quenching from the β phase and by further aging were experimentally investigated.

2. Experimental procedures

Co–21 and –23 at.% Al alloys were prepared from Co (99.9 wt.%) and Al (99.7 wt.%) by induction melting under an Ar atmosphere. Co–21 and –23 at.% Al ingots were cut into sheets about 5 mm thick (sample A and sample B, respectively) and a specimen of Co–23 at.% Al with a thickness of 1 mm was also prepared (sample C). These samples were sealed in quartz tubes evacuated and backfilled with Ar gas. Solution heat treatment was carried out at 1380 °C for 1 h, followed by quenching in ice water. For some specimens, aging heat treatments were subsequently carried out by heating from room temperature (RT) at heating rates of 5 and 10 °C/min. Microstructural observations were carried out by optical microscope using an etchant composed of the same ratio of HCl and HNO_3, transmission electron microscopy (TEM; JEOL JEM-2000EXII) at 200 kV and high-resolution electron microscopy (HREM; JEOL JEM-3010) at 300 kV. Thin foils for TEM and HREM were prepared by jet-polishing in a solution of 72% acetic acid, 12% ethanol, 8% ethylene glycol and 8% perchloric acid. Composition analysis was also conducted by TEM-EDS (energy dispersive X-ray spectroscopy), and the crystal structures of the constituent

* Corresponding author at: Department of Materials Science, Graduate School of Engineering, Tohoku University, 6-6-02 Aoba Yama, Sendai, Miyagi 980-8579, Japan. Tel.: +81 22 795 7321; fax: +81 22 795 7323.

0925-8388/$ – see front matter © 2010 Elsevier B.V. All rights reserved.
doi:10.1016/j.jallcom.2010.11.130

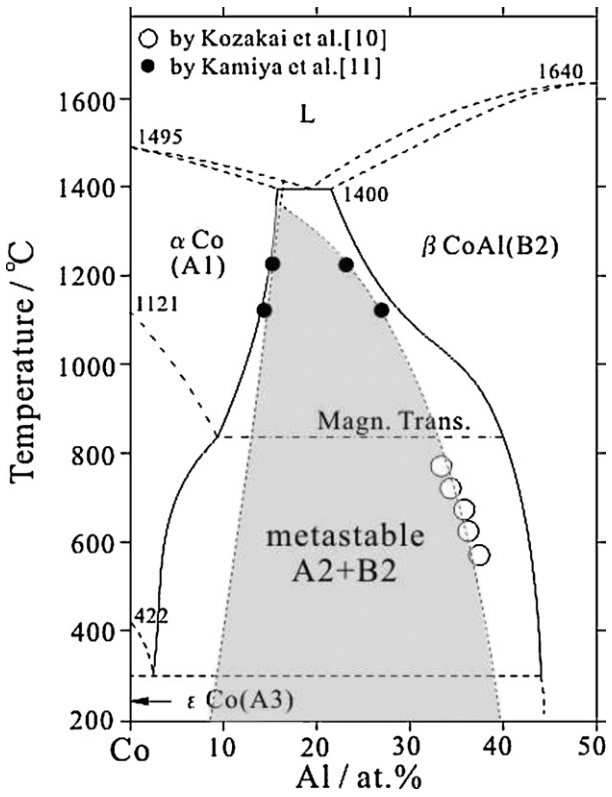

Fig. 1. Co-rich portion of Co–Al binary phase diagram including a metastable A2 + B2 two-phase region.

phases were identified by X-ray diffraction (XRD). The transformation temperatures were determined by differential scanning calorimetric (DSC) at heating rates of 1, 5 and 10 °C/min. The magnetic properties were measured by a vibrating sample magnetometer (VSM) at a heating rate of 5 °C/min.

3. Results and discussion

3.1. Martensitic and bainitic transformations

Fig. 2 shows optical micrographs of (a) sample B (5 mm in thickness), (b) sample C (1 mm in thickness) and (c) the bright field image (BFI) from the $[1\,1\,0]_{bcc}$ direction of the parent phase of sample C. Here, these samples were quenched from 1380 °C. The microstructures are different between the samples with different thicknesses, which is considered to result from the difference in the quenching rate because it should be higher in the thin specimen than in the thick one. As shown in Fig. 2(a) and (b), sample B shows thin plates, while a martensite-like structure can be partially observed in sample C. Note that sample A (5 mm in thickness) showed almost the same microstructure as sample B shown in Fig. 2(a). A very fine two-phase structure resembling spinodal decomposition, as shown in Fig. 2(c), was observed in the parent phases of all samples quenched from 1380 °C, which means that this phase separation cannot be suppressed by water quenching.

Fig. 3(a) and (b) shows the BFI from the $[1\,1\,0]_{bcc}$ direction of sample A quenched from 1380 °C and the concentration profile along a horizontal line in Fig. 3(a) obtained by using TEM-EDX. The composition of the thin plate is about Co–13 at.% Al, which is clearly lower than that of the matrix, and a concentration spike of Al is formed in the β matrix zone neighboring the plate. On the other hand, a higher magnification BFI for another plate and its corresponding SADP are shown in Fig. 3(c) and (d), respectively. High density of plane defects is observed in Fig. 3(c), and the SADP of Fig. 3(e) enlarging the square region in Fig. 3(d) shows a twin relation, which suggests that these plane defects are micro-twins. It is also confirmed from Fig. 3(d) that the plate has a fcc structure. Judging from these microstructure and composition analyses, this plate would be a product of bainitic transformation including both displacive and diffusional characteristics.

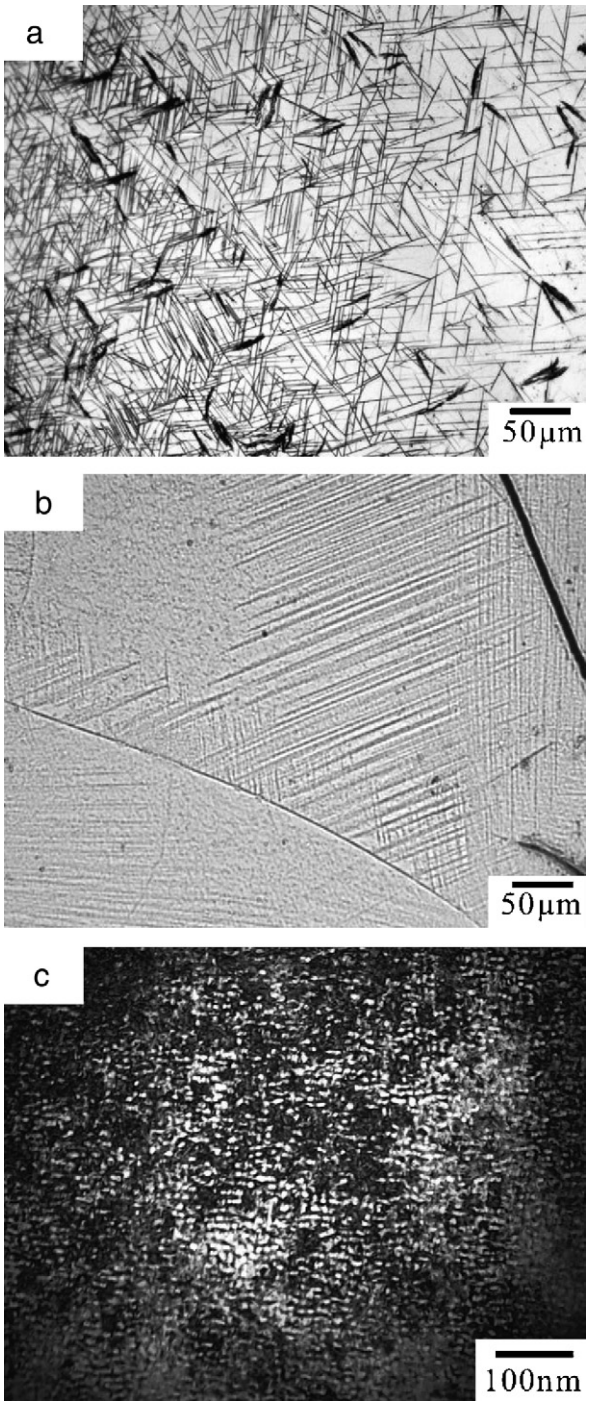

Fig. 2. Microstructures of (a) sample B (≈5 mm in thickness) and (b) sample C (≈1 mm in thickness) quenched from 1380 °C. (c) BFI taken from the $[1\,1\,0]_{bcc}$ direction of the parent phase for sample C quenched from 1380 °C.

Fig. 4 shows the BFI of the sample C quenched from 1380 °C observed in the same area of Fig. 2(b). Although a martensite-like microstructure was observed by optical microscopy, no martensite phase could be detected by TEM observation and only dislocation arrays which were probably introduced along interfaces among some martensite variants, were observed as indicated by yellow